HHS Public Access

Author manuscript

Cell Rep. Author manuscript; available in PMC 2022 December 29.

Published in final edited form as:

Cell Rep. 2022 November 22; 41(8): 111676. doi:10.1016/j.celrep.2022.111676.

Interferon partly dictates a divergent transcriptional response in poxvirus-infected and bystander inflammatory monocytes

Carolina R. Melo-Silva[1], **Marisa I. Roman**[2], **Cory J. Knudson**[1,3], **Lingjuan Tang**[1], **Ren-Huan Xu**[4], **Michel Tassetto**[5], **Patrick Dolan**[5,6], **Raul Andino**[5], **Luis J. Sigal**[1,7,*]

[1]Department of Microbiology and Immunology, Thomas Jefferson University, Philadelphia, PA 19107, USA

[2]Department of Physics, St. Joseph University, Philadelphia PA 19131, USA

[3]GlaxoSmithKline, 1250 S. Collegeville Road, Collegeville, PA 19426, USA

[4]Advanced RNA Vaccine Technologies, Inc., 12358 Parklawn Dr, North Bethesda, MD 20852, USA

[5]Department of Microbiology and Immunology, University of California San Francisco, San Francisco, CA 94158, USA

[6]Laboratory of Viral Diseases, NIAID, NIH, Bethesda, MD 20892-3210, USA

[7]Lead contact

SUMMARY

Inflammatory monocytes (iMOs) and B cells are the main targets of the poxvirus ectromelia virus (ECTV) in the lymph nodes of mice and play distinct roles in surviving the infection. Infected and bystander iMOs control ECTV's systemic spread, preventing early death, while B cells make antibodies that eliminate ECTV. Our work demonstrates that within an infected animal that survives ECTV infection, intrinsic and bystander infection of iMOs and B cells differentially control the transcription of genes important for immune cell function and, perhaps, cell identity. Bystander cells upregulate metabolism, antigen presentation, and interferon-stimulated genes. Infected cells downregulate many cell-type-specific genes and upregulate transcripts typical of non-immune cells. Bystander (Bys) and infected (Inf) iMOs non-redundantly contribute to the cytokine milieu and the interferon response. Furthermore, we uncover how type I interferon

*Correspondence: luis.sigal@jefferson.edu.

AUTHOR CONTRIBUTIONS

C.R.M.-S. and L.J.S. conceived and designed experiments, analyzed data and results, and co-wrote the paper. C.R.M.-S. performed all experiments. L.J.S. conceived the initial idea and supervised the study. M.I.R., P.D., and C.R.M.-S. performed bioinformatics and data analysis. C.J.K. and L.T. helped with some experiments. R.-H.X. and M.T. contributed to the initial setup of the experimental system. P.D. and R.A. contributed to manuscript elaboration and discussion of results.

SUPPLEMENTAL INFORMATION

Supplemental information can be found online at https://doi.org/10.1016/j.celrep.2022.111676.

DECLARATION OF INTERESTS

The authors declare no competing interests.

INCLUSION AND DIVERSITY

One or more of the authors of this paper self-identifies as an underrepresented ethnic minority in science. We support inclusive, diverse, and equitable conduct of research.

(IFN-I) or IFN-γ signaling differentially regulates immune pathways in Inf and Bys iMOs and that, at steady state, IFN-I primes iMOs for rapid IFN-I production and antigen presentation.

Graphical abstract

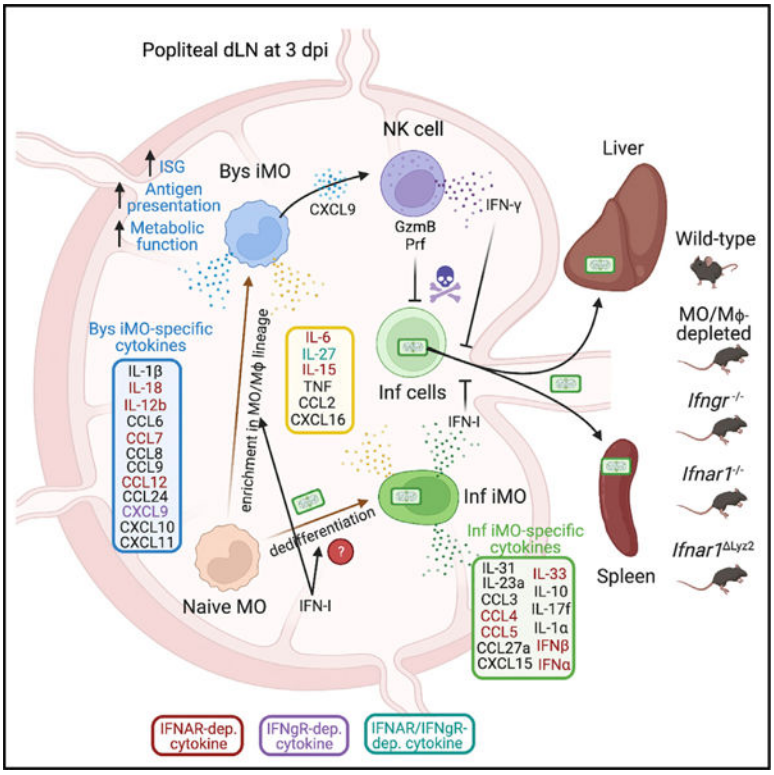

In brief

Inflammatory monocytes (iMOs) play a critical role in controlling viral spread from the draining lymph node. Melo-Silva et al. show that bystander and infected iMOs adjust their global transcription to complement each other for anti-viral protection. They also show that these transcriptional changes are partly shaped by interferon signaling.

INTRODUCTION

Numerous viruses penetrate their hosts through disruptions of epithelial surfaces, spread to the lymph nodes (LNs) that drain the site of infection (draining LNs [dLNs]) via afferent lymphatics, and become systemic by reaching the blood through efferent lymphatics. It is clear that during this process, the innate immune response in the dLN plays a major role in restraining systemic viral spread and preventing disease.[1,2]

After footpad infection, the mouse-specific orthopoxvirus ectromelia virus (ECTV) disseminates lympho-hematogenously, causing fulminant mousepox in several mouse strains such as BALB/c, but not in C57BL/6 (B6) mice, which survive without major disease partly because their innate immune response restricts the early dissemination of ECTV from the dLNs.

At 2 to 3 days post-infection (dpi), inflammatory monocytes (iMOs) and B cells, which far outnumber iMOs, are the major targets of ECTV infection in the dLNs.[3] At this time, infected (Inf), but not bystander (Bys), iMOs are the major producers of type I interferon (IFN-I).[3] Conversely, Bys iMOs, but not Inf iMOs, produce the chemokine CXCL9, which is necessary for recruiting natural killer (NK) cells to the dLNs.[4] IFN-I and NK cells, which kill Inf cells and produce critical IFN-gamma (IFN-γ), are necessary to contain the rapid dissemination of ECTV from the dLNs to the liver and the spleen. Mice depleted of MOs/macrophages with clodronate liposomes or deficient in IFN-γ, the IFN-γ receptor (*Ifngr*$^{-/-}$), or the IFNAR1 subunit (*Ifnar1*$^{-/-}$) of the IFN-I receptor (IFNAR) succumb to ECTV infection (Figure 1A).[3,5,6] Lyz2-Cre *Ifnar1*$^{fl/fl}$ mice, lacking IFNAR1 in MOs and macrophages but not in other cells, also die from ECTV infection, and their iMOs do not transcribe IFN-I efficiently.[7] To produce CXCL9, Bys iMOs need to intrinsically express the IFN-γ receptor (IFNGR).[4] Thus, iMOs require intrinsic IFNAR and IFNGR signaling to contribute to ECTV control.

B cells are also critical to resisting ECTV infection because the antibodies they produce at later stages of infection are needed for ECTV clearance.[6,8] However, B cells do not produce IFN-I or CXCL9 in response to ECTV infection.[3,4] Hence, while both iMOs and B cells are ECTV targets and essential for resistance to mousepox, Inf and Bys iMOs, but not B cells, seem to play unique and complementary roles in the early control of ECTV spread. The data also suggest that iMOs and B cells respond differently to direct and bystander infection. Here, we compared the transcriptomes of iMOs and B cells with intrinsic and bystander ECTV infection to better understand why iMOs, but not B cells, may contribute to innate immune protection.

RESULTS

Infection status defines the transcriptional profile of iMOs and B cells *in vivo*

We infected B6 mice with ECTV-expressing green fluorescent protein (ECTV-GFP). At 3 dpi, we fluorescence-activated cell sorted (FACS) Inf (GFP^{+}) and Bys (GFP^{-}) iMOs (CD11b^{high}Ly6-c^{high}) and B cells (CD19^{+}) from pooled dLNs. As controls, we sorted Ly6C^{high} iMOs from the spleen (in naive mice, iMOs are absent in LNs, and few are present in the blood) and LN B cells from uninfected (naive) mice. We extracted total RNA, made cDNA libraries, and performed RNA sequencing (RNA-seq). We selected 3 dpi because only at this time point is the number of iMOs in the dLNs at its peak;[3] the number of Inf cells is sufficient to experiment, and the innate immune response curbs ECTV dissemination from the dLNs to target organs (Figure 1B). B cells comprise most of the cells in the dLNs. Thus, the frequency of Inf B cells was lower than that of Inf iMOs (Figure 1B), but the number of Inf B cells was higher than that of Inf iMOs (Figure 1C). The infection status was confirmed by quantifying viral transcripts (Figure 1D).

Principal-component analysis (PCA) (Figure 1E) showed that Bys and naive classes clustered mainly according to cell type and subclustered according to their naive or Bys status. In contrast, Inf iMO and B cells strongly deviated from their Bys and naive counterparts. Notably, the Euclidean distance (ED) between Inf iMOs and Inf B cells was shorter than the ED between Inf and naive B cells or between Inf and naive iMOs. Class-

prediction gene clustering (Figure 1F) also showed that Inf cells strongly deviated from their naive and Bys counterparts, although they maintained their cell-type identity. Hence, the most robust changes in the transcriptional profile were caused by intrinsic infection, deviating the global transcription of iMOs and B cells away from those corresponding to their cell type.

The ED between iMOs was greater than between B cell classes (Figure 1E). Thus, the transcriptional response was stronger in iMOs than in B cells. Consistently, compared with their naive counterparts, Inf and Bys iMOs had more differentially expressed genes (DEGs) (≥2-fold change, $p < 0.01$) than Inf or Bys B cells (Figures S1A–S1F; Table S1). Inf iMOs and B cells had more DEGs than their Bys counterparts. Inf iMOs had 1,782 increased and 1,850 decreased transcripts compared with naive iMOs (Figures S1E and S1F). Hence, rather than cellular RNA depletion, as in HeLa cells infected with vaccinia virus,[9] iMOs infected *in vivo* switched their transcription to a new gene set. Only 4.2% of upregulated and 34% of downregulated DEGs in Inf iMOs belonged to pathways in the Reactome Pathways Database (RPD) (https://reactome.org), suggesting poor curation of the cellular pathways induced by intrinsic viral infection of immune cells *in vivo*.

About 50% of the DEGs in B cells were DEGs in iMOs, but only 20% of DEGs in iMOs were DEGs in B cells. The 357 upregulated and 363 downregulated genes shared between Bys and Inf iMOs represented only ~20% of DEGs in Inf iMOs but >50% of DEGs in Bys iMOs (Figures S1E and S1F). Inf and Bys B cells shared only 36 upregulated and 16 downregulated DEGs (Figures S1E and S1F). The four experimental classes shared only 11 upregulated and 2 downregulated DEGs (Figures S1E and S1F; Table S1). Class prediction analysis identified relatively large clusters of genes predominantly or uniquely expressed by Bys B cells, Bys iMOs, Inf B cells, or Inf iMOs (Figures S1K–S1N). Together, these data further show that the transcriptional response is stronger in iMOs than in B cells and in Inf than in Bys iMOs.

A direct comparison of Bys versus Inf B cells demonstrated higher transcription of 1,647 DEG in Bys and 1,454 DEGs in Inf B cells (Figure 1G). Gene Ontology (GO) analysis showed that the main cellular pathways associated with transcripts enriched in the two classes did not overlap (Figure 1H).

We have shown that Inf iMOs upregulate IFN-I genes,[3] while Bys iMOs upregulate CXCL9 transcription and translation in an IFNGR-dependent manner.[4] Comparison of Bys and Inf iMOs confirmed these results. We also identified 2,441 and 2,328 DEGs, respectively, higher in Bys or Inf iMOs (Figure 1I). As with B cells, there was no pathway overlap between the two classes by GO analysis (Figure 1J).

We used ‘‘gene set enrichment analysis’’ (GSEA) with the ‘‘Molecular Signatures Database (MsigDB) hallmark gene set collection’’ (https://www.gsea-msigdb.org) to identify cellular pathways specific for Inf versus Bys status. Bys B cells and iMOs were enriched in transcripts for the gene sets ‘‘IFN-α and IFN-γ response,’’ ‘‘glycolysis,’’ ‘‘adipogenesis,’’ and ‘‘reactive oxygen species production’’ (Figure 1K; Tables S2-3 and S2-5). Inf B cells and iMOs were enriched in transcripts for only a few gene sets (Tables S2-4 and S2-6).

At p < 5%, only the ‘‘TGF-β signaling’’ set was enriched in Inf B cells and iMOs. Inf B cells were additionally enriched for ‘‘peroxisome,’’ ‘‘DNA repair,’’ and ‘‘Myc targets’’ sets. In contrast, Inf iMOs were enriched for ‘‘WNT β-catenin’’ and ‘‘TNF-α signaling via NF-κB*’’* sets. Therefore, within an Inf host, Bys and Inf iMOs and B cells adjust their transcriptome according to their infection status, with minor overlap. The transcriptional response to intrinsic or bystander infection is greater in iMOs than in B cells. The data also suggest that in an Inf animal, Bys iMOs and B cells increase their metabolism and activate their innate immune functions, likely becoming primed to better combat their approaching intrinsic infection.

Bys cells increase, while Inf cells decrease, prototypical transcripts

We confirmed cell identity by the presence of transcripts for *Spi1* (PU.1), *Irf8*, *Klf4*, *Ccr2*, *Ly6c2*, and *Lyz2* in iMOs (Figure 2A, top) or *Cd19*, *Pax5*, *Ms4a1*, and immunoglobulin genes (*Ighd*, *Ighm*, and *Iglc1*) in B cells (Figure 2A, bottom). iMOs had no or low transcripts for *Ly6g*, *Siglech*, *Zbtb46*, *Ncr1*, *Trbc1*, and *Cd3e,* indicating good purity (deposited dataset). GSEA with the MSigDB cell-type C8 gene set collection indicated that, compared with naive or Inf B cells, Bys B cells were enriched in B cell prototypical gene sets such as the ‘‘Aizarani liver major histocompatibility complex (MHC) class II^+ B cells’’ set (Figure 2B). Similarly, Bys iMOs were enriched in gene sets typical of the MO/macrophage lineage, such as the ‘‘Travaglini lung classical monocyte’’ gene set, when compared with naive or Inf iMOs (Figure 2C). Interestingly, despite normal surface protein expression by flow cytometry (Figure 1B), Inf iMOs and B cells had decreased expression of several prototypical mRNAs compared with their naive and Bys counterparts (Figures 2A–2E). Inf B cells and iMOs were also enriched in transcripts found in gene sets typical of non-immune cells (Figures 2D and 2E).

Others have shown that in bone-marrow-derived and alveolar macrophages, cytomegalovirus (CMV) induced the upregulation of the transcription factor (TF) ZEB1, which activated genes within the Wnt and transforming growth factor β (TGF-β) signaling pathways to promote macrophage de-differentiation.[10] We found that during *in vivo* ECTV infection, Inf iMOs and B cells upregulated genes in the ‘‘TGF-β signaling’’ set, while only Inf iMOs upregulated some transcripts in the MSigDB ‘‘Wnt β-catenin’’ set, when compared with Bys (Table S1-4; Figures 2F and 2G). *Zeb1* was strongly transcribed in Bys and naive B cells, reduced in Inf B cells, and almost absent in all iMOs (Figure 2F). However, intrinsic ECTV infection induced the transcription of other genes within the WNT β-catenin set, such as *Notch4* in Inf iMOs and *Dvl2* in Inf iMOs and B cells, and in the TGF-β set, including *Klf10*, *Skil*, and *Tgif1* in Inf iMOs and B cells (Figure 2G). Also, compared with naive or Bys cells, Inf iMOs or B cells upregulated 87 experimentally verified TFs (Figure 2H). Hence, the transcriptional changes in iMOs and B cells caused by intrinsic ECTV infection differ from those caused by CMV because they do not require *de novo* ZEB1 synthesis. However, these changes could involve other genes in the Wnt and TGF-β pathways, such as *Dvl2*, *Notch4*, *Skil*, and *Tgif1* and also other TFs.

We next analyzed cell-type-specific gene sets with higher normalized GSEA scores in Inf compared with Bys iMOs, such as those for epithelial, muscle, glia, or neuronal cells.

However, we did not find an enriched gene set common to Inf iMOs and all those cell types (Figure 2I). Thus, the many transcripts prototypical of non-immune cells upregulated by Inf iMOs suggest that ECTV promotes dysregulated transcription and not de-differentiation.

Overall, our data indicate that during ECTV infection, prototypical MO/macrophage or B cell transcripts are enriched in Bys and decreased in Inf iMOs or B cells. Additionally, intrinsic ECTV infection causes the upregulation of transcripts prototypical of non-immune cells.

Bys iMOs and B cells upregulate antigen-presentation transcripts and IFN-stimulated genes (ISGs), while Bys and Inf iMOs upregulate transcription of different cytokine subsets

As professional antigen-presenting cells, B cells and iMOs display viral antigens in the context of MHC class I and class II molecules to, respectively, activate CD8 and CD4 T cells.[11] Classical and non-classical MHC class I molecules also activate or inhibit NK cells.[12] Clustering analysis indicated that compared with their naive counterparts, Bys B cells and iMOs broadly upregulated antigen-presenting genes. In contrast, Inf B cells and iMOs did not upregulate those genes and downregulated many of them (Figure 3A). These data are consistent with our previous observation that Inf iMOs downregulate MHC class II proteins at the cell surface.[7] Naive B cells, but not naive iMOs, transcribed genes encoding molecules involved in MHC class II antigen presentation, including those for the MHC class II molecules *H2-Aa*, *H2-Ab1*, and *H2-Eb1*, the invariant chain *Cd74*, the peptide editor *H2-Dma*, and the MHC class II transactivator *Ciita* (Figure 3A). Conversely, naive iMOs, but not naive B cells, transcribed genes involved in MHC class I antigen presentation such as *H2-D1*, *B2m*, *Psmb8*, *Psmb10*, and *Tapbp* (Figure 3A). When directly compared to their Inf counterparts, Bys B cells and, to a larger extent, Bys iMOs were enriched in many genes involved in MHC class I and class II antigen presentation (Figure 3B). These data suggest that MHC class II antigen presentation is constitutive in B cells and transcriptionally activated in iMOs. In contrast, MHC class I antigen presentation is constitutive in iMOs and transcriptionally activated in B cells in the context of bystander, but not intrinsic, infection.

We have recently shown that expression or absence of the non-classical MHC class I molecule Qa-1^b respectively protects or targets cells for NK cell killing *in vivo*. We also showed that Qa-1^b, which is encoded by *H2-T23*, is increased in Bys iMOs and decreased in Inf iMOs.[13] Consistent with this, iMOs and B cells upregulated, and Inf iMOs and B cells downregulated, *H2-T23* (Figures 3A and 3B). In addition, subsets of other non-classical MHC class I genes, whose functions are incompletely understood, were upregulated in Bys, but not in Inf, B cells or iMOs (Figures 3A and 3B).

We compared transcription of broadly defined ISGs.[14] Following IFN-I binding, IFNAR induces the transcription of ISG through downstream STAT1, STAT2, and IRF9. *Stat1* and *Stat2* were moderately transcribed in naive cells and highly upregulated in Bys, but not in Inf, cells (Figure 3C). Naive iMOs transcribed *Irf9*, which was maintained in Bys, but downregulated in Inf, iMOs. *Irf9* transcription was low in naive and Inf, but upregulated in Bys, B cells. These data suggested that Bys, but not Inf, iMOs and B cells are primed for rapid ISG transcription. Consistently, cluster analysis showed that Bys cells were the main

ISG transcribers *in vivo* (Figure 3D). Compared with naive iMOs, Bys iMOs upregulated the largest number of ISGs, followed by Bys B cells, Inf iMOs, and Inf B cells (Figure 3E; Table S1-8). Bys iMOs and Bys B cells shared as many as 71 ISGs, while only 16, 2, and 12 ISGs were shared between Bys and Inf iMOs, Bys and Inf B cells, and Inf iMOs and Inf B cells, respectively (Figure 3E). Therefore, ISGs were mostly induced in Bys cells, and most of the ISGs in B cells were a subset of those in iMOs.

Naive B cells and naive iMOs transcribed some non-overlapping ISGs (Figure 3D, clusters 1 and 2, respectively). All B cell classes transcribed most cluster 1 transcripts (Figures 3D and S2A), while most cluster 2 transcripts were downregulated in Bys and, to a greater extent, in Inf iMOs (Figures 3D and S2B). Thus, *in vivo*, bystander or intrinsic infection can induce the downregulation of some genes thought to be ISGs.

We compared the transcription of genes important for resistance to mousepox. B6 mice deficient in either *Irf7*, *Nfkb1*, *Tmem173*, *Myd88*, *Cgas*, or *Tlr9* are highly susceptible to ECTV.[3,4,15,16] *Irf7*, *Nfkb1*, *Tmem173*, *Myd88*, *Cgas*, and *Tlr9* were prominently upregulated in Bys, but not in Inf, iMOs. Only *Nfkb1*, which is necessary for IFN-β transcription,[3] was upregulated in Inf and not in Bys iMOs (Figure 3F). B cells had a similar trend but with much lower expression levels. This likely explains why Inf B cells do not transcribe IFN-I[3] and as shown below.

We compared the effects of intrinsic or bystander infection in the transcription of IFN genes. Naive iMOs or B cells did not transcribe IFN-I (Figure 3G). Unlike naive and Bys iMOs, Inf iMOs upregulated *Ifnb1* and multiple *Ifna* genes. Compared with naive iMOs, Bys iMOs upregulated transcripts for *Ifnb1* and *Ifna4* but much less so than Inf iMOs. Thus, the transcription of IFN-I during *in vivo* viral infection has strong cell-type and infection status specificity. We have previously shown that IFN-I transcription depends on the TFs *Irf7* and *Nfkb1*.[3] We now find that *Irf7* is upregulated in Bys and *Nfkb1* in Inf iMOs (Figure 3F). Thus, NF-kB likely initiates IFN-I transcription in Inf cells, while IRF7 requires *de novo* synthesis triggered by the IFNAR positive feedback loop.[7]

We analyzed the transcription of other cytokines (Figures 3H–3J). Naive iMOs constitutively transcribed interleukins *Il17c*, *Il18*, *Il1b*, *Il15*, and *Il16* and chemokines *Ccl6* and *Ccl9*. Compared with naive iMOs, both Inf and Bys iMOs downregulated *Il16*, *Ccl6*, and *Ccl9* and upregulated six cytokines: *Il27*, *Il6*, *Tnf*, *Cxcl16*, and *Ccl2* ($p < 0.001$ for both groups for all genes). Notably, cytokine transcripts were largely absent in B cells, except for *Il12a* and *Il16*, which all B cells classes transcribed, and *Il23a* ($p < 0.001$), which was transcribed only by Inf B cells. We next compared Bys and Inf iMOs (Figure 3J). Eleven cytokines were expressed significantly higher in Bys iMOs: *Il1b*, *Il18*, *Il12b*, *Ccl6*, *Ccl9*, *Ccl8* ($p = 0.05$), *Ccl12*, *Ccl24*, *Cxcl9*, *Cxcl10*, and *Cxcl11*. *Ccl7* did not reach significance ($p = 0.06$), likely due to Inf iMO variability. Inf iMOs expressed significantly more *Ifnb1*, multiple *Ifna*, and 11 additional cytokines: *Il31*, *Il33*, *Il23a*, *Il1a*, *Il10*, *Il17f*, *Ccl27a*, *Ccl5*, *Ccl4*, *Ccl3*, and *Cxcl15*. *Ifnar1* was upregulated in Inf iMOs, while *Ifnar2*, *Ifngr1*, and *Ifngr2* transcription was similar in Inf and Bys iMOs (Figure 3J).

The data in this section show that Bys cells are primed for antigen presentation and ISG upregulation and that Inf and Bys iMOs, but not B cells, transcribe large, mostly non-overlapping cytokines subsets. These data suggest that Inf and Bys iMOs complement each other in producing cytokines during the early immune response in the dLNs.

Infection status, and not IFN signaling, defines the overall transcriptional response of iMOs

Given the critical roles of IFNAR and IFNGR in resistance to ECTV[5,17,18] and the need for IFNAR in Lyz2^{+} cells to resist mousepox,[7] we next analyzed how intrinsic IFNAR or IFNGR deficiency affected the transcriptional changes induced in iMOs by intrinsic of bystander ECTV infection. We made congenically marked, mixed bone marrow chimeras (BMCs) by lethally irradiating wild-type (WT) B6-*Cd45*$^{2/2}$ mice and reconstituting them with a mixture of bone marrow cells from WT B6-*CD45*$^{1/1}$ and mutant B6-*CD45*$^{2/2}$*Ifnar1*$^{-/-}$ (*Ifnar1*$^{-/-}$) or B6-*CD45*$^{2/2}$*Ifngr*$^{-/-}$ (*Ifngr*$^{-/-}$) mice to generate WT + *Ifnar1*$^{-/-}$→WT and WT + *Ifngr*$^{-/-}$→WT BMCs (Figure 4A). In these BMCs, WT and mutant iMOs in the dLNs are exposed to the same microenvironment and virus loads. After infecting the BMCs with ECTV-GFP, we sorted Bys and Inf WT and *Ifnar1*$^{-/-}$ or *Ifngr*$^{-/-}$ iMOs (CD11b^{high}Ly6C^{high}, sorting strategy as in Figure 1B) from the dLNs at 3 dpi. Naive WT and mutant iMOs were sorted from the spleen of naive BMC as controls. RNA-seq was performed as before.

Class prediction clustering and PCA (Figures 4B and 4C) showed that the overall transcriptional profile first separated the cells according to their infection status rather than their genotype. Still, as described below, many effects on cellular pathways and DEGs observed in the previous sections were due to IFN signaling.

Compared with naive WT, naive *Ifnar1*$^{-/-}$ iMOs downregulated 89 and upregulated 18 genes (Figure S3A; Table S3-1). The main GO pathways affected by the lack of IFNAR in naive iMOs were ‘‘immune system,’’ ‘‘cytokine signaling,’’ and ‘‘IFN-I signaling’’ (Figure S3B). Interestingly, naive *Ifnar1*$^{-/-}$ iMOs had lower expression of *Irf7*, *Stat2*, and *Irf9* (Figure S3C), suggesting that, at steady state, iMOs need IFNAR not only to respond to but also to produce basal levels of IFN-I. Among the numerous downregulated genes, many were ISGs, including *Oas1g*, *Ifi213*, and *Siglec1* (Figure S3D). Different from naive *Ifnar1*$^{-/-}$ iMOs, naive *Ifngr*$^{-/-}$ iMOs only downregulated 10 and upregulated 6 transcripts (Figures S3E and S3F; Table S3-2). None of the genes downregulated in naive *Ifngr*$^{-/-}$ iMOs were known ISGs, suggesting that there may not be basal levels of IFN-γ signaling at steady state and that activation of this pathway might require inflammation. Thus, at steady state, IFNAR, but not IFNGR, signaling poises naive iMOs to a more responsive antiviral state.

Compared with WT iMOs, *Ifnar1*$^{-/-}$ Bys iMOs had 33 genes with increased and 182 genes with decreased transcription (Figure 4D; Table S3-3). The most prominent pathways decreased in Bys *Ifnar1*$^{-/-}$ iMOs were ‘‘immune system,’’ ‘‘cytokine signaling,’’ and ‘‘IFN-I signaling.’’ At the same time, the few genes that had increased transcription were associated with ‘‘granulopoiesis,’’ ‘‘IL-4 and IL-13 signaling,’’ and ‘‘IL-10 signaling’’ (Figure 4E).

Compared with WT iMOs, *Ifngr*$^{-/-}$ Bys iMOs had 86 increased and 241 decreased mRNAs (Figure 4F; Tables S3-4). The main pathways disrupted in *Ifngr*$^{-/-}$ Bys iMOs were ''IFN-II-induced ISG'' and ''extracellular protein interactions'' (Figure 4G). Surprisingly, only 8.3% of downregulated transcripts were associated with known pathways in the RPD, indicating an underrepresentation of IFNGR-dependent pathways or a lack of available data.

Compared with WT iMOs, *Ifnar1*$^{-/-}$ Inf iMOs had 51 increased and 191 decreased transcripts (Figures 4H, Table S3-5). The few increased mRNAs in Inf *Ifnar1*$^{-/-}$ iMOs were involved in ''neutrophil degranulation,'' ''cyclin S phase,'' and IL-10 signaling''. In contrast, most of the many decreased transcripts were related to ''immune system,'' ''cytokine signaling,'' ''IFN-I signaling,'' ''megakaryocyte development,'' and ''IRF7 activation'' (Figure 4I).

Compared with WT iMOs, *Ifngr*$^{-/-}$ Inf iMOs had 62 increased and 73 decreased mRNAs (Figures 4J; Table S3-6). Some increased transcripts were associated with ''post-translational protein phosphorylation'' and ''DNA replication,'' while some of those decreased corresponded with the ''unfolded protein response'' (Figure 4K).

IFNAR1 and IFNGR are partly and non-redundantly responsible for the changes induced by ECTV in Bys iMOs

As shown above, antigen-presentation genes were predominantly transcribed by Bys iMOs (Figure 3A). Surprisingly, IFN signaling had only a partial effect on the upregulation of genes involved in MHC class I and very little or no effect on MHC class II antigen-presentation genes (Figures 5A and 5B). IFNGR had a significant role in the upregulation of transcripts for the immunoproteasome subunit *Psmb9*, the TAP peptide transporter subunit *Tap2*, the Tapasin-like protein (*Tapbpl*), and various non-classical MHC class I genes. Changes in *Tap1* (fold change = 0.75) and Tapasin (*Tapbp*; fold change = 0.62) did not reach statistical significance. IFNAR1 was necessary for the efficient upregulation of *B2m*, *H2-Eb2*, and several non-classical MHC class I genes.

We showed above that Bys iMOs presented robust ISG upregulation (Figure 3D). As expected, Bys *Ifnar1*$^{-/-}$ and *Ifngr*$^{-/-}$ iMOs had reduced upregulation of multiple ISGs (Figure 5C; Tables S3-7). From the 126 ISG upregulated in Bys iMO sorted from B6 mice (Figures 3H), 123 were also upregulated in Bys WT iMO sorted from the mixed BMC (Figure 5D), demonstrating the reliability of the results. Of these, 44 (~36%) required IFNAR1, including ISG important for resistance to mousepox such as *cGas* and *Irf7*; 31 (~25%) required IFNGR, including *Stat1* and *Irf1*, 13 (~10.6%) required both IFNAR and IFNGR, and 35 (~28%) did not require either IFNAR or IFNGR, suggesting redundant roles of IFN-I and IFN-γ, or IFN independence (Figure 5D and Tables S3-7). Of note, *Tlr9*, *Cgas*, and *Irf7*, but not *Tmem173* or *Myd88*, required IFNAR for efficient expression (Figure 5E), even though all of them are necessary to resist ECTV.

Bys iMOs transcribed 18 cytokines *in vivo* (Figures 3G–3I). IFNAR caused decreased upregulation of six (*Il6*, *Il12b*, *Il18*, *Il15*, *Ccl12*, and *Ccl7*) and IFNGR deficiency of only two (*Il27* and *Cxcl9*) (Figures 5F and 5G).

We also noted that Bys iMOs were enriched in iMO prototypical transcripts (Figure 2C). This enrichment was reduced in *Ifnar1*$^{-/-}$ (Figure 5H), but not in *Ifngr*$^{-/-}$, iMOs. Overall, these data indicate that IFNAR and IFNGR cooperate non-redundantly to prime Bys iMOs to respond to infection.

IFNAR1 is partly responsible for the transcriptional changes that occur in Inf MOs

We next analyzed the impact of IFNAR and IFNGR on cytokine production (Figure 6A). In agreement with our previous results,[7] IFN-I transcription required intrinsic IFNAR (Figures 6A and 6B). Of the other 15 cytokines transcribed by Inf iMOs, intrinsic IFNAR deficiency resulted in no or decreased upregulation of four (*Il6*, *Il33*, *Ccl4*, and *Ccl5*). *Il27* did not reach significance ($p = 0.06$). IFNGR deficiency had little or no effect on Inf iMO cytokine transcription (Figures 6C and 6D).

While ISGs are known to inhibit viral replication,[19] the frequency of total ECTV transcripts was not increased in *Ifnar1*$^{-/-}$ or *Ifngr*$^{-/-}$ iMOs, indicating that ISG upregulation does not restrict ECTV transcription in Inf iMOs *in vivo* (Figure 6E). Also, IFNAR or IFNGR deficiency did not alter the transcription of early, intermediate, or late ECTV genes.

Inf iMOs downregulated MO/macrophage-prototypical transcripts and upregulated mRNAs distinctive of non-immune cells (Figures 2E and 2I). Compared with Bys *Ifnar1*$^{-/-}$ or Bys *Ifngr*$^{-/-}$ iMOs, Inf *Ifnar1*$^{-/-}$ and Inf *Ifngr*$^{-/-}$ iMOs still had reduced MO/macrophage-specific transcripts (Figure S3G). Also, *Ifnar1*$^{-/-}$, but not WT or *Ifngr*$^{-/-}$, Inf iMOs obtained from BMCs failed to upregulate many of the genes we identified as specifically upregulated in Inf iMOs compared with naive in non-irradiated WT mice (Figure 6F, compare with Figure S1M and Tables S1-9). Therefore, changes in cell-prototypic transcripts induced in iMO by intrinsic infection partly depend on IFNAR but not on IFNGR signaling.

DISCUSSION

Our PCA indicates that within an animal infected with a poxvirus, the transcriptional profile of Bys iMOs and B cells is defined more by the cell's identity than by the host's infection status. On the other hand, Inf iMOs and B cells, which suffer larger transcriptional changes, are more defined by their infection status than by their cell identity, as indicated by a shorter ED between them than with their naive or Bys counterparts. The finding that Inf cells suffer this large transcriptional shift *in vivo* suggests technical implications for using unbiased sequencing approaches such as single-cell RNA-seq (scRNA-seq) of virus-infected organs. Unlike RNA-seq of sorted populations, unbiased scRNA-seq without oligo-tagged antibody (Ab) hashing may mischaracterize the identity of some cell populations. For example, Inf immune cells might be misread as non-hematopoietic or immune cell progenitors.

In addition to losing prototypical transcripts, Inf iMOs and B cells gained transcripts typical of non-immune cells. Others recently made a similar observation for alveolar macrophages infected with CMV.[10] Thus, our experiments suggest that transcriptional dysregulation may be a common cellular response to intrinsic viral infection. Unlike CMV-infected macrophages, ECTV-infected iMOs and B cells did not upregulate *Zeb1* but upregulated other Wnt and TGF-β genes previously described as involved in cellular transformation

or differentiation[20–23] and a large set of TFs. Future studies to investigate whether these genes play a role in the transcriptional dysregulation induced by intrinsic ECTV infection could be important because, in other models, it has been shown that Inf cells' transcriptional changes can affect viral replication and disease.[10,24–26] Notably, our data also indicate that many of the transcriptional changes observed in Inf iMOs were partly dependent on IFNAR, indicating that IFN-I contributes to the transcriptional profile of Inf cells.

Very few Inf versus naive or Bys cell DEGs were associated with cellular pathways curated in public databases. This suggests that the pathways activated by intrinsic viral infection are not well studied. Our data contribute to filling this knowledge gap and can be used as a reference for transcriptional signatures of immune cells infected with poxviruses *in vivo*.

The responses of Bys cells were very different from those of their Inf counterparts. Bys iMOs and B cells were enriched in transcripts typical of their cell types and upregulated mRNAs for molecules required to present antigen. IFNAR and IFNGR non-overlappingly contributed to the transcription of genes important for MHC class I, but not for MHC class II, antigen presentation. IFNGR deficiency decreased the upregulation of genes involved in antigen processing and peptide transport. IFNAR deficiency resulted in inefficient upregulation of transcripts for *b2m*, which is a critical component of classical and non-classical MHC class I molecules. Yet, IFNGR or IFNAR deficiency did not fully abrogate the upregulation of any of these transcripts, suggesting that IFN-I and IFN-γ have overlapping effects or that IFN acts in concert with other cytokines or signaling pathways to boost antigen presentation. Most importantly, the data suggest that Bys cells are primed to rapidly present antigens if they become infected. On the other hand, Inf iMOs and B cells transcribed little or no transcripts for antigen-presentation genes, suggesting a shutdown in antigen processing and presentation, a short time window for antigen presentation after intrinsic infection, and a transition to increased vulnerability to NK cell killing.

Our data also show that intrinsic IFNAR and IFNGR regulate ISG transcription non-redundantly. Out of all the ISGs upregulated in Bys iMOs, ~36% were dependent on IFNAR, ~25% on IFNGR, ~28% were upregulated redundantly or independent of IFN, and 10.6% required both IFNAR and IFNGR.

We have already defined many of the mechanisms involved in IFN-I induction following *in vivo* ECTV infection. Efficient transcription of all IFN-I subtypes requires the pathogen recognition receptor cGAS,[16] which produces cGAMP to activate STING. Downstream, the efficient transcription of IFN-β and IFN-α requires NF-κB or IRF7, respectively.[3] Unlike in Bys WT iMOs, *Cgas* and *Irf7* were not upregulated in *Ifnar1*$^{-/-}$ Bys iMOs. Thus, their upregulation requires IFN-I. These data suggest that the first set of Inf cells produce low levels of IFN-β in an NF-κB-dependent manner. This initial IFN-β likely primes Bys iMOs to produce all IFN-I subtypes more efficiently as they become infected. Mechanistically, this model fits the high susceptibility to ECTV observed in *Nfkb1*$^{-/-}$-, *Cgas*$^{-/-}$-, and *Irf7*$^{-/-}$-deficient mice[15,16] and the observation that ECTV-infected *Ifnar1*$^{-/-}$ mice can still transcribe IFN-I genes.[16]

Remarkably, IFN-I, but not IFN-γ, was indispensable for *Tlr9* transcription, whereas *Myd88* and *Tmem173* transcription was IFN independent or IFN redundant. In addition, Bys cells increased transcripts that define the MO/macrophage lineage in an IFNAR-dependent, but IFNGR-independent, manner. Thus, IFN-I primes many of the anti-viral functions in Bys iMOs.

Notably, Inf and Bys iMOs transcribed large numbers of cytokines. Inf iMOs transcribed IFN-I (*Ifnb1* and multiple *Ifna*) and 15 additional cytokines, while Bys iMOs only minimally upregulated IFN-I but upregulated transcripts for 18 cytokines. Only six cytokines were shared by Inf and Bys iMOs. Thus, Inf and Bys iMOs, but not B cells, seem to have mostly non-redundant and complementary roles in shaping the cytokine milieu of the dLNs. These data suggest that resistance to viral infection may require an ideal ratio of Bys/Inf iMOs to shape the early immune response. In support, we have previously found that the frequencies of Inf iMOs are increased in the dLNs of mousepox-susceptible mice such as *Cgas*$^{-/-}$[16] and aged mice.[27] Of the 16 cytokines transcribed by Inf iMOs, five were IFNAR dependent, and none were IFNGR dependent. Of the 18 cytokines expressed by Bys iMOs, six required IFNAR, and two required IFNGR. Therefore, IFN-I, to a great extent, and IFN-γ, to a lesser extent, partially, but not fully, control the transcription of cytokines in iMOs.

The observation that *Ifnar1*$^{-/-}$ naive iMOs downregulate *Irf7*, *Irf9*, *Siglec1*, and other immune-related genes agrees with previous observations that IFN-I induced by microbiota at steady state poise conventional dendritic cells for IFN-I production.[28] Hence, our studies expand the notion that IFN-I primes myeloid cells at a steady state to rapidly respond to infection.

Many ISGs are known for their direct antiviral functions.[19] However, the frequencies of total viral transcripts in WT, *Ifnar1*$^{-/-}$, or *Ifngr*$^{-/-}$ Inf iMOs did not differ. We recently reported similar results for WT and *Ifnar1*$^{-/-}$ iMOs using qPCR and ECTV plaque assay.[7] Hence, at least for ECTV, the impact of IFN on Inf cell transcription primarily targets the regulation of the immune response rather than the reduction of viral transcripts.

Our work collectively demonstrates that in the dLNs of an Inf animal whose immune system efficiently controls a viral disease, intrinsic and bystander infection differentially control the transcription of genes important for immune cell function and, perhaps, cell identity. Our data indicate that Bys and Inf iMOs non-redundantly contribute to the cytokine milieu and the IFN response. Furthermore, our work uncovered how IFN-I or IFN-γ signaling differentially regulate immune pathways in Inf and Bys iMOs and shows that, at a steady state *in vivo*, IFN-I primes iMOs for rapid IFN-I production and antigen presentation after infection.

Limitations of the study

A caveat to our BMC experimental setup is that *Ifnar1*$^{-/-}$ and *Ifngr*$^{-/-}$ iMOs could not be separated from the ~5% residual, WT-host-derived iMOs.[7] Thus, minor changes between WT and mutant iMOs could have been overlooked.

STAR★METHODS

RESOURCE AVAILABILITY

Lead contact—Further information and requests for resources and reagents should be directed to Luis J. Sigal (Luis.Sigal@jefferson.edu) or Carolina Melo-Silva (Carolina.Rezende.Melo.da.Silva@jefferson.edu).

Materials availability—This study did not generate new unique reagents.

Data and code availability

- Raw and processed mRNA-Seq data are available in the Gene Expression Omnibus (GEO) under series entry GSE215747.
- This paper does not report original code;
- Any additional information required to reanalyze the data reported in this paper is available from the lead contact upon request.

EXPERIMENTAL MODEL AND SUBJECT DETAILS

All mice used for viral infection were 8–12 weeks old or 16 to 18 weeks old for BMC. To make BMC, we used 4 to 6 weeks old females. We used only females because in our experience, male BMC fight and usually kill each other or get bad fighting wounds. C57BL/6NCrl (B6) and B6.SJL-*Ptprc*^{a}*Pepc*^{b}/BoyCrl (CD45.1) mice were purchased from Charles River directly for experiments or as breeders. *Ifnar1*$^{-/-}$ mice backcrossed to B6 were gifts from Dr. Thomas Moran (Mount Sinai School of Medicine, New York, NY). B6.129S7-Ifngr1^{tm1Agt}/J (*Ifngr*$^{-/-}$) mice were purchased from the Jackson Laboratory. Colonies were bred at Thomas Jefferson University under specific pathogen-free conditions. Mice were group housed on individually ventilated cages and fed on 5010 LabDiet. All mice procedures were carried out according to the Eighth Edition of the Guide for the Care and Use of Laboratory Animals of the National Research Council of the National Academies. All experiments were approved by Thomas Jefferson University's Institutional Animal Care and Use Committee under protocol number 01727, "Innate Control of Viral Infections." Library preparation from a few cells/single cell protocol was selected to reduce the number of animals required for each experiment in order to adhere to ARRIVE guidelines in the reduction category.

METHOD DETAILS

Viruses and infection—ECTV-GFP[29] was propagated in tissue culture, as previously described.[7] Briefly, BS-C-1 cells grown in DMEM media supplemented with 10% fetal bovine serum (FBS), 100 IU penicillin, 100 μg/mL streptomycin, 1x GlutaMAX, and 10mM HEPES to confluency were Inf at MOI 0.01, and viruses were harvested 4 to 5 days later. Cells were rinsed with phosphate-buffered solution (PBS), scraped, and concentrated by centrifugation. ECTV was released by multiple freezing and thawing cycles. Virus stocks were sonicated and titrated by plaque assay in BS-C-1 cells. Mice were infected subcutaneously in both rear footpads with 3000 plaque-forming units (PFU) per footpad of ECTV-GFP.

Bone marrow chimeras (BMC)—4- to 6-week-old mice previously treated for three days with acidified water (pH 2.5) were irradiated with 9 Gy using a GammaCell 40 apparatus (Nordion Inc.). Bone marrow cells were isolated in RPMI media supplemented with 10% FBS, 100 IU/mL penicillin, and 100 μg/mL streptomycin. Red blood cells were lysed with 0.84% NH_4Cl and cells were filtered and counted. Irradiated mice were reconstituted intravenously with 10 million bone marrow cells from donors. BMC animals were given acidified water for four weeks and rested eight weeks after reconstitution.

Flow cytometry and sorting—Groups of 5 B6 mice or 8–10 BMC were Inf with 3000 pfu of ECTV-GFP in the footpad. At three dpi, bystander (Bys, GFP^-) and infected (Inf, GFP^+) B-cells and iMO were sorted from the popliteal dLNs. Sorted samples correspond to a pool of 10 popliteal dLN from 5 B6 infected mice or 16–20 popliteal dLN from 8 to 10 BMC or one naive spleen or LN. dLN were treated with Liberase TM (1.67 Wünsch units/mL) for 30 min in PBS supplemented with 10mM HEPES. Single-cell suspensions were passed through a 70μm strainer, and repetitive washes with PBS supplemented with 2% BSA and 10mM HEPES. Spleen from one naive mouse was used for sorting naive iMO. Spleens were smashed with frosted slides, and cells were washed with RPMI media supplemented with 10% FBS, 100 IU/mL penicillin, and 100 μg/mL streptomycin. Red blood cells were lysed with 0.84% NH_4Cl. Cells were treated with anti-mouse CD16/CD32 (0.25mL per million cells) for 15 min at 4°C in PBS supplemented with 2% BSA and 1mM EDTA and subsequently stained with surface antibodies for 20 min at 4°C. Cells were washed and sorted with a FACSAria II sorter in PBS supplemented with 1% BSA, 25mM HEPES, and 1mM EDTA. Sorting data were analyzed with FlowJo version 10.

RNA and library preparation and RNA sequencing—B-cells and iMO were sorted directly into Trizol. Total RNA was purified with the RNA Clean and Concentrator with DNase I treatment (Zymo Research), and RNA was eluted in 10mL. RNA purification was quantified by Qubit, and quality control was performed by RIN analysis (High Sensitivity RNA Screen Tape – Agilent) by the SKKC Metaomics Facility at Thomas Jefferson University. 1ng or 100pg of total RNA was used for library preparation with the mouse Ovation SoLo RNA-Seq Systems, including DNaseI and Insert-Dependent Adaptor Cleavage (InDA-C) treatments for DNA and rRNA depletion. Final libraries were run on Hiseq Illumina PE150 by Novogene. For B cell and iMO sorted from B6-Inf animals, three biological replicates of each population (Bys, Inf, and Naive) were sequenced, except for B cell Inf for which only two biological replicates were sequenced. For WT, *Ifnar1*$^{-/-}$ and *Ifngr*$^{-/-}$ iMO sorted from Inf BMCs, four biological replicates were sequenced for Bys and Inf WT iMO, and two biological replicates were sequenced for each Bys and Inf knockout iMO.

QUANTIFICATION AND STATISTICAL ANALYSIS

High-throughput sequencing reads were analyzed pseudo alignment with *Mus Musculus* GRCm38.p6 and ECTV Moscow GCA_000841905.1 genomes using Kallisto (v0.46.1).[30] Transcript abundance was normalized to transcript per million, and differential expression (DE) was calculated using the Sleuth R package (v0.30.0).[31] *pval <0.05, **pval <0.01, ***pval <0.001 and ****pval <0.0001. DEG was defined as those presenting at least a 2-

fold change and p value (pval) < 0.01. PCA based on ED was generated with the R package version 4.1.2. DEG volcano plots (2-fold change and p < 0.01, unless indicated otherwise) were generated with the VolcaNoseR online tool.[37] Clustering heatmap of correlations of centered and scaled transcript values and class comparison prediction analysis were generated in Biometric Research Program BRB- ArrayTools (2-fold change, p < 0.01, ≥10 transcripts per million in at least one experimental group).[32] Venn diagrams of DEG were generated using the JVenn plug-in.[33] GO analyses were performed on DEG with a p < 0.05 filter on selected pathways of the RPD.[34] GSEA analysis was performed using C8 (cell type signature gene sets) and H (hallmark gene sets) collections (http://www.gsea-msigdb.org/gsea/msigdb/collections.jsp), in which Sigal2Noise or diff_of_classes analysis were employed for ranking genes in phenotype analysis for 1000 iterations.[35,36] Result analysis includes gene sets enriched (adjusted enrichment score – NES) at nominal pval <5% and false discovery rate (qval FDR) preferably below 0.25. ISG list was compiled from genes described in the literature in mouse and human cell studies (Table S2-7).[14,19,38] TF list of experimentally verified TF was derived from the Cancer Genome Anatomy Project (http://cgap.nci.nih.gov/Pathways). The iMO-specific class prediction gene list was derived from Table S1-9. Data were analyzed with Prism 8 Software and bar graphs show mean ± SEM.

Supplementary Material

Refer to Web version on PubMed Central for supplementary material.

ACKNOWLEDGMENTS

This work was supported by grants R56AI110457 and R01AI110457 to L.J.S. and R01AI16946002 to R.A. and L.J.S., all from NIAID, and AAI Careers in Immunology Fellowship partially supported C.R.M.-S. T32 AI134646 from NIAID supported C.J.K. The present research utilized the Flow Cytometry, Metaomics, and Laboratory Animal facilities at SKCC at Jefferson Health (supported by NCI-P30CA056036).

REFERENCES

1. Kastenmüller W, Torabi-Parizi P, Subramanian N, Lämmermann T, and Germain RN (2012). A spatially-organized multicellular innate immune response in lymph nodes limits systemic pathogen spread. Cell 150, 1235–1248. 10.1016/j.cell.2012.07.021. [PubMed: 22980983]
2. Wong E, Montoya B, Stotesbury C, Ferez M, Xu RH, and Sigal LJ (2019). Langerhans cells orchestrate the protective antiviral innate immune response in the lymph node. Cell Rep 29, 3047–3059.e3, e3043. 10.1016/j.celrep.2019.10.118. [PubMed: 31801072]
3. Xu RH, Wong EB, Rubio D, Roscoe F, Ma X, Nair S, Remakus S, Schwendener R, John S, Shlomchik M, and Sigal LJ (2015). Sequential activation of two pathogen-sensing pathways required for type I interferon expression and resistance to an acute DNA virus infection. Immunity 43, 1148–1159. 10.1016/j.immuni.2015.11.015. [PubMed: 26682986]
4. Wong E, Xu RH, Rubio D, Lev A, Stotesbury C, Fang M, and Sigal LJ (2018). Migratory dendritic cells, group 1 innate lymphoid cells, and inflammatory monocytes collaborate to recruit NK cells to the virus-infected lymph node. Cell Rep 24, 142–154. 10.1016/j.celrep.2018.06.004. [PubMed: 29972776]
5. Panchanathan V, Chaudhri G, and Karupiah G (2005). Interferon function is not required for recovery from a secondary poxvirus infection. Proc. Natl. Acad. Sci. USA 102, 12921–12926. 10.1073/pnas.0505180102. [PubMed: 16123129]

6. Chaudhri G, Panchanathan V, Bluethmann H, and Karupiah G (2006). Obligatory requirement for antibody in recovery from a primary poxvirus infection. J. Virol 80, 6339–6344. 10.1128/jvi.00116-06. [PubMed: 16775322]
7. Melo-Silva CR, Alves-Peixoto P, Heath N, Tang L, Montoya B, Knudson CJ, Stotesbury C, Ferez M, Wong E, and Sigal LJ (2021). Resistance to lethal ectromelia virus infection requires Type I interferon receptor in natural killer cells and monocytes but not in adaptive immune or parenchymal cells. Plos Pathog 17, e1009593. 10.1371/journal.ppat.1009593. [PubMed: 34015056]
8. Fang M, and Sigal LJ (2005). Antibodies and CD8+ T cells are complementary and essential for natural resistance to a highly lethal cytopathic virus. J. Immunol 175, 6829–6836. 10.4049/jimmunol.175.10.6829. [PubMed: 16272340]
9. Dai A, Cao S, Dhungel P, Luan Y, Liu Y, Xie Z, and Yang Z (2017). Ribosome profiling reveals translational upregulation of cellular oxidative phosphorylation mRNAs during vaccinia virus-induced host shutoff. J. Virol 91, 018588–e1916. 10.1128/jvi.01858-16.
10. Baasch S, Giansanti P, Kolter J, Riedl A, Forde AJ, Runge S, Zenke S, Elling R, Halenius A, Brabletz S, et al. (2021). Cytomegalovirus subverts macrophage identity. Cell 184, 3774–3793.e25, e3725. 10.1016/j.cell.2021.05.009. [PubMed: 34115982]
11. Rock KL, Reits E, and Neefjes J (2016). Present yourself! By MHC class I and MHC class II molecules. Trends Immunol 37, 724–737. 10.1016/j.it.2016.08.010. [PubMed: 27614798]
12. Sun JC, and Lanier LL (2011). NK cell development, homeostasis and function: parallels with $CD8^+$ T cells. Nat. Rev. Immunol 11, 645–657. 10.1038/nri3044. [PubMed: 21869816]
13. Ferez M, Knudson CJ, Lev A, Wong EB, Alves-Peixoto P, Tang L, Stotesbury C, and Sigal LJ (2021). Viral infection modulates Qa-1b in infected and bystander cells to properly direct NK cell killing. J. Exp. Med 218, e20201782. 10.1084/jem.20201782. [PubMed: 33765134]
14. Schoggins JW, Wilson SJ, Panis M, Murphy MY, Jones CT, Bieniasz P, and Rice CM (2011). A diverse range of gene products are effectors of the type I interferon antiviral response. Nature 472, 481–485. 10.1038/nature09907. [PubMed: 21478870]
15. Rubio D, Xu RH, Remakus S, Krouse TE, Truckenmiller ME, Thapa RJ, Balachandran S, Alcamí A, Norbury CC, and Sigal LJ (2013). Crosstalk between the type 1 interferon and nuclear factor kappa B pathways confers resistance to a lethal virus infection. Cell Host Microbe 13, 701–710. 10.1016/j.chom.2013.04.015. [PubMed: 23768494]
16. Wong EB, Montoya B, Ferez M, Stotesbury C, and Sigal LJ (2019). Resistance to ectromelia virus infection requires cGAS in bone marrow-derived cells which can be bypassed with cGAMP therapy. Plos Pathog 15, e1008239. 10.1371/journal.ppat.1008239. [PubMed: 31877196]
17. Remakus S, and Sigal LJ (2011). Gamma interferon and perforin control the strength, but not the hierarchy, of immunodominance of an antiviral CD8+ T cell response. J. Virol 85, 12578–12584. 10.1128/jvi.05334-11. [PubMed: 21917955]
18. Xu RH, Cohen M, Tang Y, Lazear E, Whitbeck JC, Eisenberg RJ, Cohen GH, and Sigal LJ (2008). The orthopoxvirus type I IFN binding protein is essential for virulence and an effective target for vaccination. J. Exp. Med 205, 981–992. 10.1084/jem.20071854. [PubMed: 18391063]
19. Schneider WM, Chevillotte MD, and Rice CM (2014). Interferon-stimulated genes: a complex web of host defenses. Annu. Rev. Immunol 32, 513–545. 10.1146/annurev-immunol-032713-120231. [PubMed: 24555472]
20. Uyttendaele H, Closson V, Wu G, Roux F, Weinmaster G, and Kitajewski J (2000). Notch4 and Jagged-1 induce microvessel differentiation of rat brain endothelial cells. Microvasc. Res 60, 91–103. 10.1006/mvre.2000.2254. [PubMed: 10964583]
21. Yamaguchi Y, Naiki T, and Irie K (2012). Stau1 regulates Dvl2 expression during myoblast differentiation. Biochem. Biophys. Res. Commun 417, 427–432. 10.1016/j.bbrc.2011.11.133. [PubMed: 22166206]
22. Wara AK, Foo S, Croce K, Sun X, Icli B, Tesmenitsky Y, Esen F, Lee JS, Subramaniam M, Spelsberg TC, et al. (2011). TGF-β1 signaling and Krüppel-like factor 10 regulate bone marrow-derived proangiogenic cell differentiation, function, and neovascularization. Blood 118, 6450–6460. 10.1182/blood-2011-06-363713. [PubMed: 21828131]
23. Tecalco-Cruz AC, Ríos-López DG, Vázquez-Victorio G, Rosales-Alvarez RE, and Macías-Silva M (2018). Transcriptional cofactors Ski and SnoN are major regulators of the TGF-β/Smad signaling

pathway in health and disease. Signal Transduct. Target. Ther 3, 15. 10.1038/s41392-018-0015-8. [PubMed: 29892481]

24. Barbian HJ, Seaton MS, Narasipura SD, Wallace J, Rajan R, Sha BE, and Al-Harthi L (2022). β-catenin regulates HIV latency and modulates HIV reactivation. Plos Pathog 18, e1010354. 10.1371/journal.ppat.1010354. [PubMed: 35255110]
25. Denney L, Branchett W, Gregory LG, Oliver RA, and Lloyd CM (2018). Epithelial-derived TGF-β1 acts as a pro-viral factor in the lung during influenza A infection. Mucosal Immunol 11, 523–535. 10.1038/mi.2017.77. [PubMed: 29067998]
26. Hargest V, Bub T, Neale G, and Schultz-Cherry S (2022). Astrovirus-induced epithelial-mesenchymal transition via activated TGF-β increases viral replication. Plos Pathog 18, e1009716. 10.1371/journal.ppat.1009716. [PubMed: 35452499]
27. Stotesbury C, Wong EB, Tang L, Montoya B, Knudson CJ, Melo-Silva CR, and Sigal LJ (2020). Defective early innate immune response to ectromelia virus in the draining lymph nodes of aged mice due to impaired dendritic cell accumulation. Aging Cell 19, e13170. 10.1111/acel.13170. [PubMed: 32657004]
28. Schaupp L, Muth S, Rogell L, Kofoed-Branzk M, Melchior F, Lienenklaus S, Ganal-Vonarburg SC, Klein M, Guendel F, Hain T, et al. (2020). Microbiota-induced type I interferons instruct a poised basal state of dendritic cells. Cell 181, 1080–1096.e19, e1019. 10.1016/j.cell.2020.04.022. [PubMed: 32380006]
29. Fang M, Lanier LL, and Sigal LJ (2008). A role for NKG2D in NK cell-mediated resistance to poxvirus disease. Plos Pathog 4, e30. 10.1371/journal.ppat.0040030. [PubMed: 18266471]
30. Bray NL, Pimentel H, Melsted P, and Pachter L (2016). Near-optimal probabilistic RNA-seq quantification. Nat. Biotechnol 34, 525–527. 10.1038/nbt.3519. [PubMed: 27043002]
31. Pimentel H, Bray NL, Puente S, Melsted P, and Pachter L (2017). Differential analysis of RNA-seq incorporating quantification uncertainty. Nat. Methods 14, 687–690. 10.1038/nmeth.4324. [PubMed: 28581496]
32. Simon R, Lam A, Li MC, Ngan M, Menenzes S, and Zhao Y (2007). Analysis of gene expression data using BRB-ArrayTools. Cancer Inform 3, 11–17. [PubMed: 19455231]
33. Bardou P, Mariette J, Escudié F, Djemiel C, and Klopp C (2014). jvenn: an interactive Venn diagram viewer. BMC Bioinformatics 15, 293. 10.1186/1471-2105-15-293. [PubMed: 25176396]
34. Fabregat A, Sidiropoulos K, Viteri G, Forner O, Marin-Garcia P, Arnau V, D'Eustachio P, Stein L, and Hermjakob H (2017). Reactome pathway analysis: a high-performance in-memory approach. BMC Bioinformatics 18, 142. 10.1186/s12859-017-1559-2. [PubMed: 28249561]
35. Mootha VK, Lindgren CM, Eriksson KF, Subramanian A, Sihag S, Lehar J, Puigserver P, Carlsson E, Ridderstråle M, Laurila E, et al. (2003). PGC-1alpha-responsive genes involved in oxidative phosphorylation are coordinately downregulated in human diabetes. Nat. Genet 34, 267–273. 10.1038/ng1180. [PubMed: 12808457]
36. Subramanian A, Tamayo P, Mootha VK, Mukherjee S, Ebert BL, Gillette MA, Paulovich A, Pomeroy SL, Golub TR, Lander ES, and Mesirov JP (2005). Gene set enrichment analysis: a knowledge-based approach for interpreting genome-wide expression profiles. Proc. Natl. Acad. Sci. USA 102, 15545–15550. 10.1073/pnas.0506580102. [PubMed: 16199517]
37. Goedhart J, and Luijsterburg MS (2020). VolcaNoseR is a web app for creating, exploring, labeling and sharing volcano plots. Sci. Rep 10, 20560. 10.1038/s41598-020-76603-3. [PubMed: 33239692]
38. Tretina K, Park ES, Maminska A, and MacMicking JD (2019). Interferon-induced guanylate-binding proteins: guardians of host defense in health and disease. J. Exp. Med 216, 482–500. 10.1084/jem.20182031. [PubMed: 30755454]

Highlights

- Bys and Inf iMOs and B lymphocytes have different transcriptional profiles *in vivo*
- Bys cells upregulate cell-type-specific, antigen-presentation, and ISG transcripts
- Bys and Inf iMOs transcribe large non-overlapping cytokine sets
- IFN-I and IFN-γ non-redundantly dictate cytokine transcription in Bys and Inf iMOs

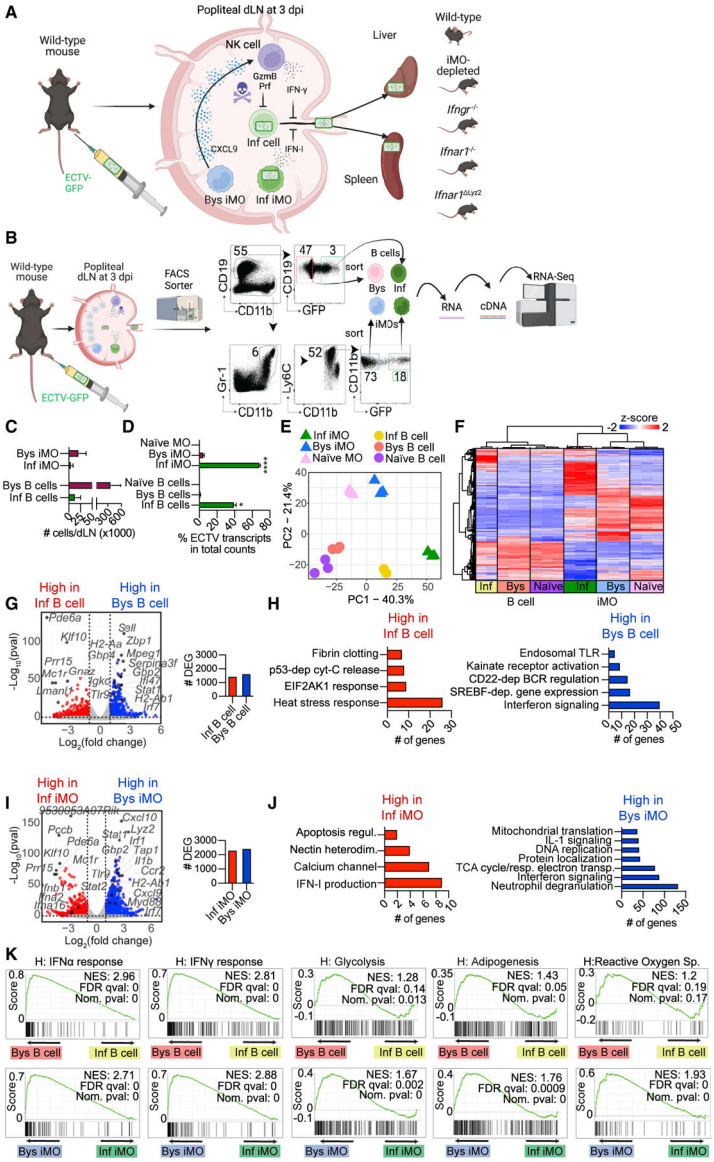

Figure 1. Infection status defines the transcriptional profile of iMOs and B cells *in vivo*

(A) Innate immune response in the dLNs at 3 dpi reduces virus dissemination and promotes host survival (BioRender.com).

(B) At 3 dpi, Bys and Inf B cells ($CD19^{+}$) and iMOs ($CD11b^{high}Ly6C^{high}$) were sorted from the popliteal dLNs of ECTV-infected animals, and their transcriptional profile was determined by RNA-seq (BioRender.com).

(C) Number of each sorted population from the dLNs of infected mice.

(D) Frequencies of ECTV transcripts in total read counts. p value (pval) determined by Student's t test analysis between Inf and Bys groups.

(E) ED PCA.

(F) Clustering heatmap of class-predicting genes.

(G) Volcano plot and graph show the number of DEGs expressed higher in Inf or Bys B cells.

(H) GO based on the RPD of genes transcribed in Inf and Bys B cells.
(I) Volcano plot and graph showing the number of DEGs expressed higher in Inf or Bys iMOs.
(J) GO based on the RPD of genes transcribed in Inf and Bys iMOs.
(K) GSEA of cellular pathways (MSigDB H) in Bys versus Inf B cells (top, enriched in Bys B cells) or Bys versus Inf iMOs (bottom, enriched in Bys iMOs).
Three biological replicates of each sorted population (Bys, Inf, and naive) were sequenced, except for Inf B cells, for which only two biological replicates were sequenced. Each biological replicate is derived from a pool of 10 popliteal dLNs from 5 B6 infected mice or one naive spleen (naive iMOs) or LN (naive B cells). Error bars represent the standard error of the mean.

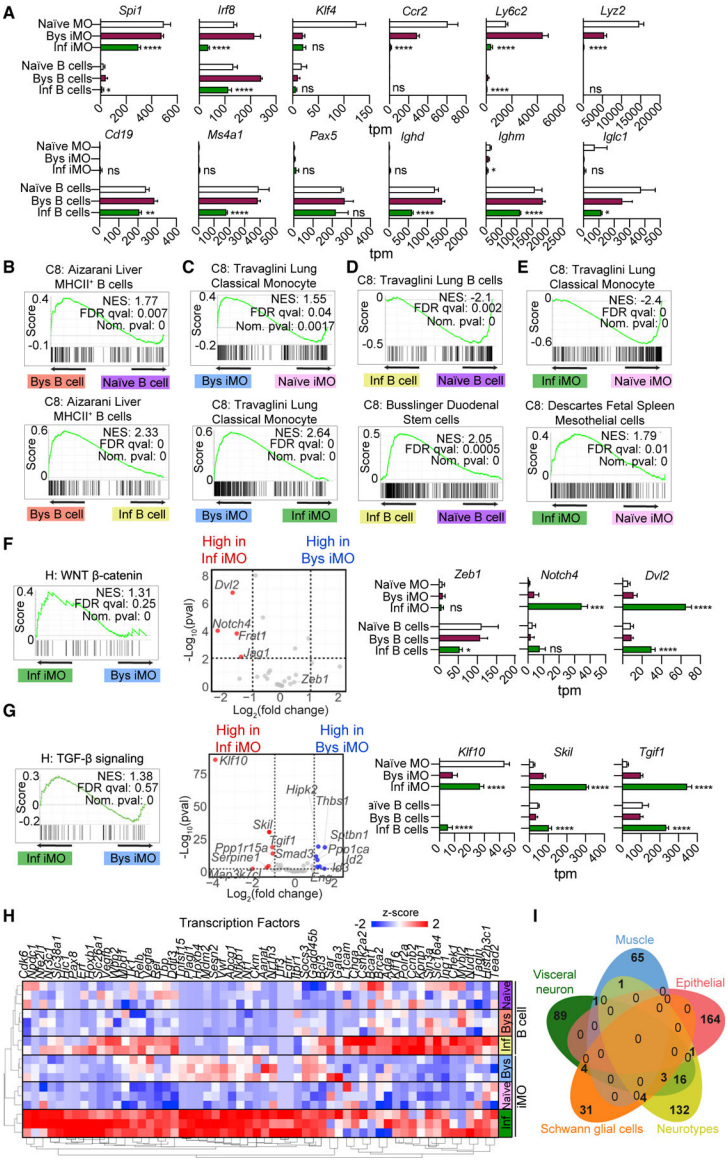

Figure 2. Bys cells increase, while Inf cells decrease, prototypical transcripts

(A) Transcription levels of iMO (top) or B cell (bottom) specific markers in sorted cells. pval determined by DE-sleuth analysis between Inf and Bys groups.

(B) GSEA enrichment in Bys B cells in B cell gene set (MSigDB C8) compared with naive B cells (top, enrichment in Bys B cells) or Inf B cells (bottom, enrichment in Bys B cells).

(C) GSEA enrichment in Bys iMOs in myeloid cells gene set (MSigDB C8) compared with naive iMOs (top, enrichment in Bys iMOs) or in monocyte gene set (MSigDB C8) compared with Inf iMOs (bottom, enrichment in Bys iMOs).

(D) GSEA enrichment (MSigDB C8) in Inf B cells compared with naive B cells in B cell gene set (top, enrichment in naive B cells) and stem cell gene set (bottom, enrichment in Inf B cells).

(E) GSEA enrichment (MSigDB C8) in Inf iMOs compared with naive iMO in monocyte gene set (top, enrichment in naive iMOs) or mesothelial cell gene set (bottom, enrichment in Inf iMOs).

(F and G) GSEA enrichment (MSigDB H), volcano plot, and graphs of the WNT β-catenin gene set (F) and the TGF-β signaling gene set (G) of Inf iMOs compared with Bys iMOs (enrichment in Inf iMOs). pval determined by DE-sleuth analysis between Inf and Bys groups.

(H) Clustering heatmap of experimentally verified TF transcripts increased in Inf populations.

(I) Venn diagram depicting unique and shared Inf iMO-correlated transcripts from MSigDB C8 gene sets with positive enrichment for Inf iMOs. Samples correspond to those in Figure 1. pval determined by DE-sleuth analysis between Inf and Bys groups. Error bars represent the standard error of the mean.

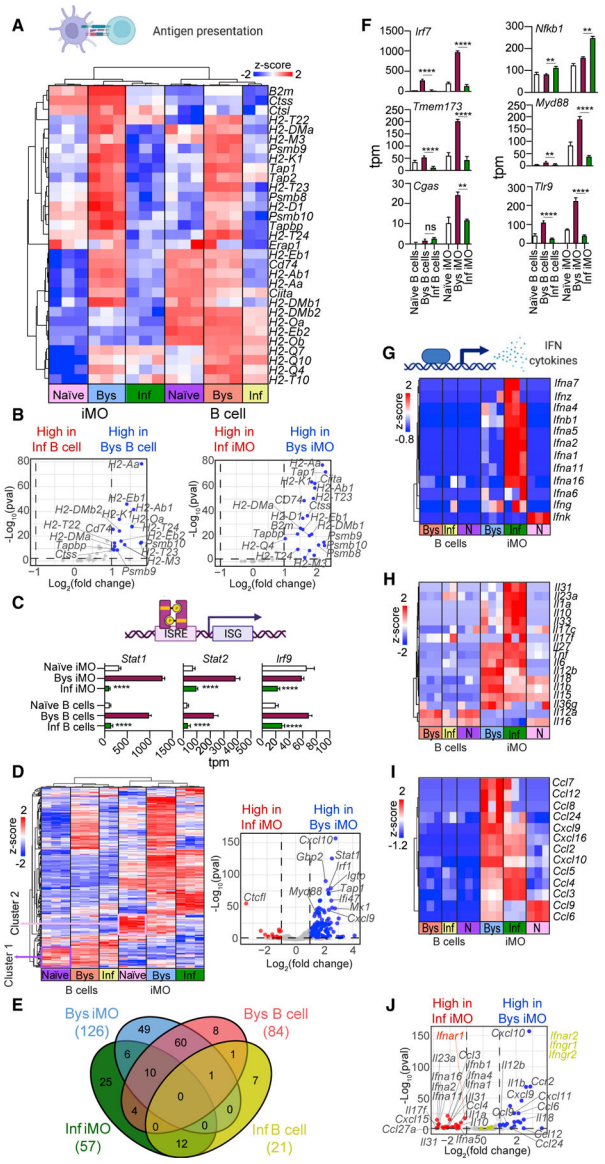

Figure 3. Bys iMOs and B cells upregulate antigen-presentation transcripts and ISGs, while Bys and Inf iMOs upregulate transcription of different cytokine subsets

(A) Clustering heatmap of transcripts for antigen-presenting genes.

(B) Volcano plot comparing antigen-presenting gene transcription in Bys versus Inf cells. Bys versus Inf B cells (left) and Bys versus Inf iMOs (right).

(C) Transcript levels of TF genes responsible for ISG upregulation, i.e., Stat1, Stat2, and Irf9 genes.

(D) Clustering heatmap of ISGs and volcano plot comparing ISG transcription in Bys iMOs versus Inf iMOs. Cluster 1 highlights ISGs constitutively transcribed in naive B cells and cluster 2 ISGs constitutively transcribed in naive iMOs.

(E) Venn diagram depicting unique and shared ISG transcripts increased compared with naive.

(F) Transcript levels of Irf7, Tmem173, Cgas, Nfkb1, Myd88, and Tlr9.

(G–I) Clustering heatmap of IFN (G), interleukin (H), and chemokine (I) genes.

(J) Volcano plot comparing cytokine transcription in Bys versus Inf iMOs (2-fold change and $p < 0.05$). Samples correspond to those in Figure 1. pval determined by DE-sleuth analysis between Inf and Bys groups. Error bars represent the standard error of the mean.

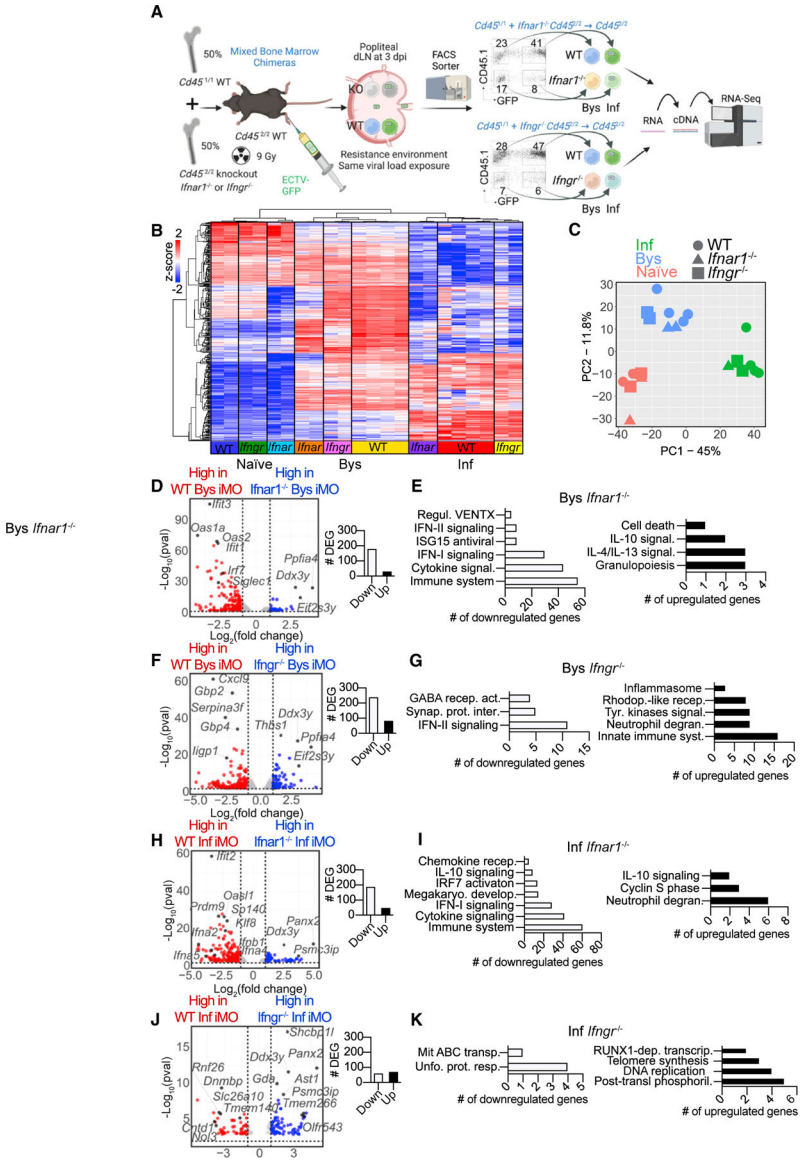

Figure 4. Infection status, and not IFN signaling, defines the overall transcriptional response of iMO

(A) Bys WT, *Ifnar1*$^{-/-}$, and *Ifngr*$^{-/-}$ iMOs and Inf WT, *Ifnar1*$^{-/-}$, and *Ifngr*$^{-/-}$ iMOs were sorted from dLNs of B6.CD45$^{1/1}$ + *Ifnar1*$^{-/-}$ CD45$^{2/2}$→B6.CD45$^{2/2}$ and B6.CD45$^{1/1}$ + *Ifngr*$^{-/-}$CD45$^{2/2}$→B6.CD45$^{2/2}$ ECTV-infected BMCs at 3 dpi, as in Figure 1B, and their transcriptional profile determined by RNA-seq (BioRender.com).

(B and C) Clustering heatmap (B) and PCA analysis (C) of iMO-specific class predicting transcripts.

(D and E) Volcano plot showing DEGs (D) and GO based on the RPD (E) of increased or decreased transcripts in Bys *Ifnar1*$^{-/-}$ iMOs compared with Bys WT iMOs.

(F and G) Volcano plot showing DEGs (F) and GO based on the RPD (G) of increased or decreased transcripts in Bys *Ifngr*$^{-/-}$ iMOs compared with Bys WT iMOs.

(H and I) Volcano plot showing DEGs (H) and GO based on the RPD (I) of increased or decreased transcripts in Inf *Ifnar1*$^{-/-}$ iMOs compared with Inf WT iMOs.

(J and K) Volcano plot showing DEGs (J) and GO based on the RPD (K) of increased or decreased transcripts in Inf *Ifngr*$^{-/-}$ iMOs compared with Inf WT iMOs.
Four biological replicates were sequenced for Bys and Inf WT iMOs, and two biological replicates were sequenced for naive WT iMOs and for each naive, Bys, and Inf knockout iMO. Each biological replicate is derived from a pool of 16–20 popliteal dLNs from 8 to 10 infected BMCs or one spleen from 1 naive BMC. pval determined by DE-sleuth analysis between WT and knockout groups.

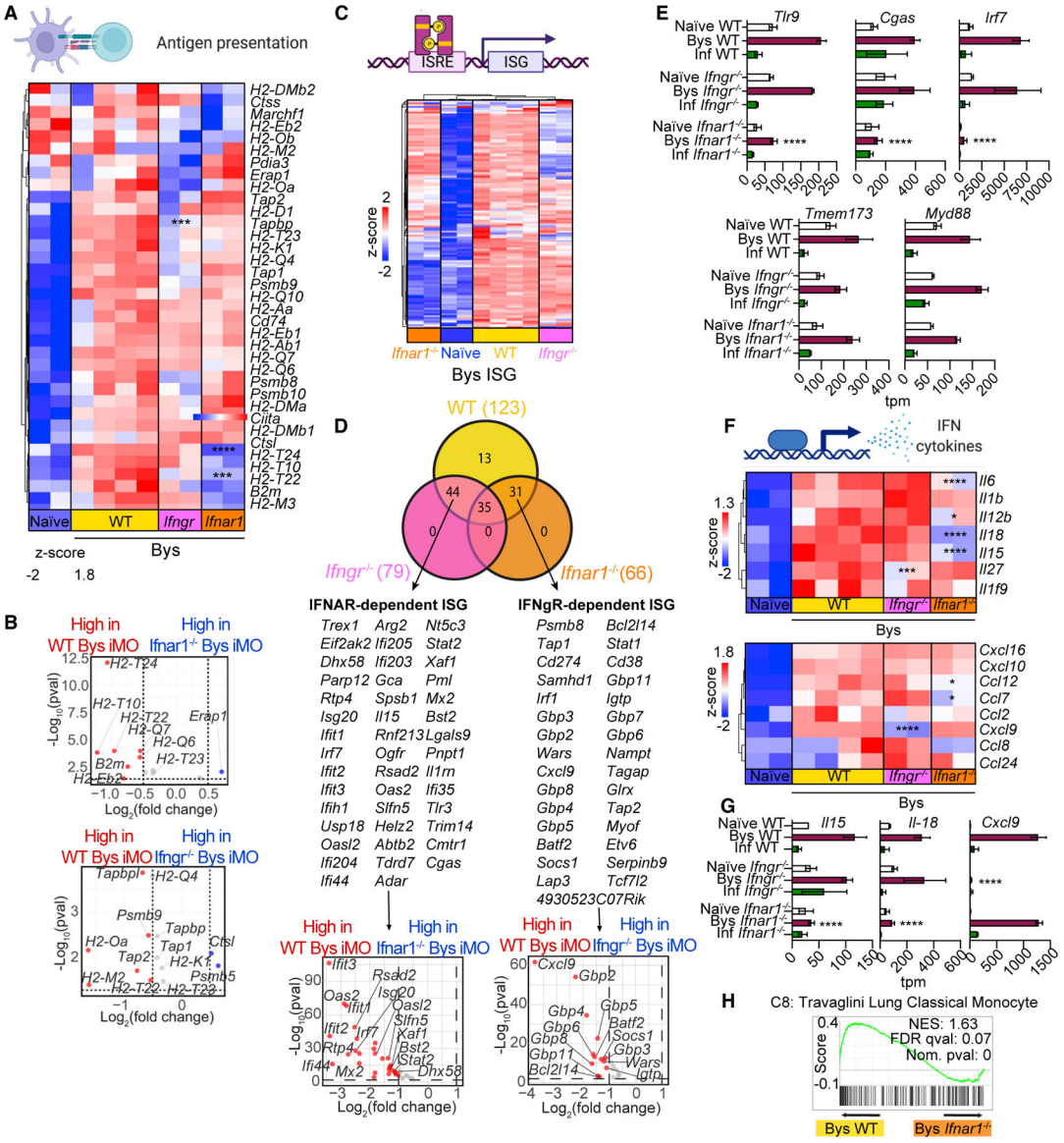

Figure 5. IFNAR1 and IFNGR are partly and non-redundantly responsible for the changes induced by ECTV in Bys iMOs

(A) Clustering heatmap of transcripts for molecules involved in antigen presentation.

(B) Volcano plot of antigen-presentation genes in the indicated Bys iMOs (1.4-fold change and $p < 0.05$).

(C) Clustering heatmap of ISGs.

(D) Venn diagram depicting unique and shared ISGs among Bys populations and volcano plot of IFNAR-dependent ISGs (left) and IFNGR-dependent ISGs (right) in the indicated Bys iMOs.

(E) Transcript levels of *Tlr9*, *Cgas*, *Irf7*, *Tmem173*, and *Myd88*.

(F) Clustering heatmap of cytokine transcripts specifically upregulated in Bys iMOs.

(G) Transcript levels of cytokine genes affected by either *Ifnar1*$^{-/-}$ or *Ifngr*$^{-/-}$ deletion in Bys iMOs.

(H) GSEA enrichment in Bys WT iMOs in Travaglini lung classical monocyte gene set (MSigDB C8) compared with Bys *Ifnar1*$^{-/-}$ iMOs. Samples correspond to those in Figure 4. pval determined by DE-sleuth analysis between WT and knockout groups. Error bars represent the standard error of the mean.

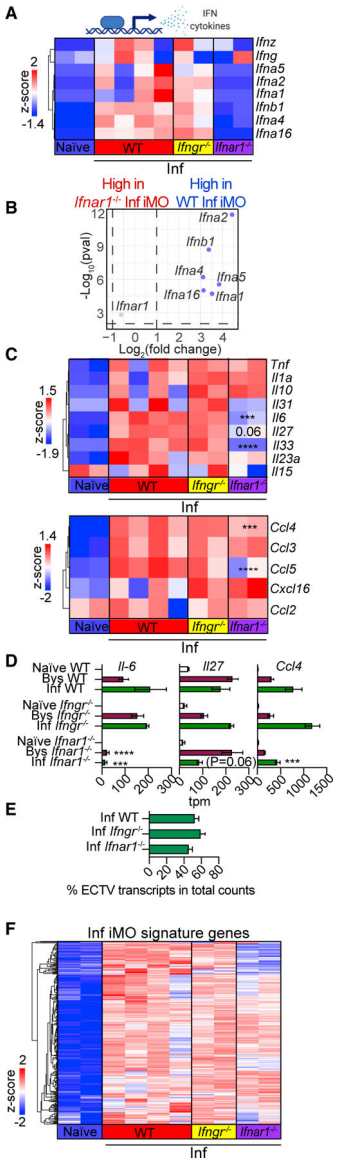

Figure 6. IFNAR1 is partly responsible for the transcriptional changes that occur in Inf MOs

(A and B) Clustering heatmap (A) and volcano plot (B) of the indicated IFN transcripts in the indicated iMOs.

(C and D) Clustering heatmap (C) and transcript levels (D) of cytokine genes specifically increased in Inf WT iMOs.

(E) Frequencies of ECTV transcripts in total counts of each Inf population.

(F) Clustering heatmap of genes specifically increased Inf iMOs. Samples correspond to those in Figure 4. pval determined by DE-sleuth analysis between WT and knockout groups. Error bars represent the standard error of the mean.

KEY RESOURCES TABLE

REAGENT or RESOURCE	SOURCE	IDENTIFIER
Antibodies		
Mouse monoclonal antibody BV785 anti-mouse CD45.1, clone A20	BioLegend	Cat# 110743, RRID:AB_2563379
Rat monoclonal antibody BUV395 anti-mouse CD11b, clone M1/70	BD Biosciences	Cat# 565976, RRID:AB_2721166
Rat monoclonal antibody PE anti-mouse Ly6C, clone HK1.4	BioLegend	Cat# 128008, RRID:AB_1186132
Rat monoclonal antibody Pacific Blue anti-mouse Ly6C/Ly6G (Gr-1), clone RB6–8C5	BioLegend	Cat# 108430, RRID:AB_893556
Rat monoclonal antibody BV785 anti-mouse CD19, clone 6D5	BioLegend	Cat# 115543, RRID:AB_11218994
Rat monoclonal antibody anti-mouse CD16/CD32, clone 93	BioLegend	Cat#101302; RRID:AB_312801
Bacterial and virus strains		
ECTV-GFP	Fang et al.[29]	N/A
Chemicals, peptides, and recombinant proteins		
DMEM media	CORNING	10–013-CV
RPMI media	CORNING	10–040-CV
Penicillin Streptomycin Solution, 100x	CORNING	30–002-Cl
Fetal Bovine Serum, Heat Inactivated	Seradigm	1500–500
GlutaMAX 100x	Gibco	35,050–061
HEPES 1M	CORNING	25–060-Cl
Liberase™	Roche	05,401 119,001
Critical commercial assays		
mouse Ovation SoLo RNA-Seq Systems	NuGEN	0501
RNA Clean and Concentrator™-5	Zymo Research	R1014
Experimental models: Cell lines		
Monkey *C. aethiops* epithelial kidney BS-C-1 cells	ATCC	CCL-26
Experimental models: Organisms/strains		
Mouse: C57BL/6NCrl	Charles River	027
Mouse: B6.SJL-*Ptprc*^{a}*Pepc*^{b}/BoyCrl	Charles River	494
Mouse: C57BL/6 *Ifnar1*$^{-/-}$ mice	Thomas Moran (Mount Sinai School of Medicine, New York, NY)	N/A
Mouse: B6.129S7-Ifngr1^{tm1Agt}/J	Jackson Laboratory	JAX: 003,288
Software and algorithms		
Kallisto	Bray et al.[30]	N/A
Sleuth	Pimentel et al.[31]	N/A
BRB-ArrayTools	Simon et al.[32]	N/A
Jvenn	Bardou et al.[33]	N/A
Reactome Pathways Database	Fabregat et al.[34]	N/A
GSEA	Mootha et al.[35], Subramanian et al.[36]	N/A
VolcaNoseR	Goedhart et al.[37]	N/A
Prism 8 Software	GraphPad Software	N/A

REAGENT or RESOURCE	SOURCE	IDENTIFIER
FlowJo™ version 10	Treestar	N/A
Other		
FACSAria™ II sorter	BD Biosciences	N/A
Raw and processed mRNA-Seq data	GEO	GSE215747